ChemComm

COMMUNICATION

View Article Online
View Journal | View Issue

Cite this: *Chem. Commun.*, 2014, **50**, 9357

Received 12th May 2014,
Accepted 26th June 2014

DOI: 10.1039/c4cc03555k

www.rsc.org/chemcomm

A phosphomolybdic acid anion probe-based label-free, stable and simple electrochemical biosensing platform†

Tianxiang Wei, Yuyun Chen, Wenwen Tu, Yaqian Lan and Zhihui Dai*

A versatile label-free, stable, low-cost and simple electrochemical biosensing platform has been developed based on a phosphomolybdic acid anion probe by jointly taking advantages of its native electronegativity, electrochemical activity and chemisorption with graphene oxide.

Nowadays, electrochemical sensing platforms developed for the analysis of biomolecules are attracting increasing interest.[1,2] Considering the practical application, recent studies of electrochemical biosensors have focused on new designs to lower the cost, increase the stability, speed up the test, and simplify the operation processes, and so forth.[3]

Polyoxometalates (POMs) are a kind of typical early-transition-metal–oxygen-anion cluster with an almost unmatched range of properties and applications.[4] For example, POMs are often applied in the layer-by-layer assembly process by making use of electrostatic interactions due to their native electronegativity.[5] Besides, POMs have attracted more and more attention in the field of electrochemistry because of their unique electrochemical activities, among which is their reversible multi-electron redox behavior for energy storage applications.[6] Also, the strong chemisorption between carbon materials and POMs has been used to construct POM–carbon composites.[7] It would not be an exaggeration to say that POMs are a combination of lots of advantages. However, most of the researchers have used only one of its properties. Therefore, it would be reasonable to expect a combination of its gathered advantages.

Many existing electrochemical assays for DNA and proteins employ some groups to label biomolecules like complementary DNA strands and antibodies, which is inevitably accompanied by long processing times, increased operational difficulty and an increase in expense.[8] Given this, in recent years, several groups have reported label-free methods for detecting their targets by applying complex designs (*e.g.*, hand-in-hand DNA nanostructures[9a]), introducing new synthetic materials (*e.g.*, functionalized carbon nanotubes[9b]) or using special techniques (*e.g.*, impedance spectroscopy[9c]). However, most of these reported design concepts and synthetic materials always have a pretty complex process. Moreover, the reproducibility and reliability of impedance spectroscopy measurements are still open to discussion. Based on this, it can be speculated that the electrochemical activity of POMs could make themselves appropriate electrochemical signal probes. We had two considerations: first, we anticipated that electronegative POMs would repel the same charged DNA. Second, based on the different capacities of interaction of single- and double-stranded DNA with graphene oxide (GO),[10] the vacancy on the interface of GO generated by double-stranded DNA release might form a stable complex with POMs on account of its strong chemisorption on carbon materials. Herein, phosphomolybdic acid ($H_3PMo_{12}O_{40}$) was chosen as a typical representative among POMs. Using a disease-related gene sequence (mitochondrial DNA related to maternally inherited diabetes) and the thrombin as models, a versatile label-free, stable, low-cost and simple electrochemical biosensing platform was designed for bioanalysis by jointly employing three natural characteristics of $[PMo_{12}O_{40}]^{3-}$ (PMo_{12}), including its electronegativity, electrochemical activity and chemisorption with GO, for the first time.

The basic principle of the PMo_{12}-based electrochemical biosensor is shown in Scheme 1. GO was initially immobilized on a chitosan modified glassy carbon electrode (GCE/chitosan) *via* amide bonds generated by its carboxylic groups and amino groups of chitosan (see ESI,† Fig. S1).[11] Through π–π* stacking interactions between the conjugated interface of GO and DNA bases,[10] the capture DNA (single-stranded DNA or aptamer) was successfully immobilized on the GO surface. As the negatively charged capture DNA covered the surface of GO, the strong negatively charged PMo_{12} could not get access to the electrode surface owing to steric hindrance and charge repulsion. After binding with the target DNA or protein, the resulting

Jiangsu Collaborative Innovation Center of Biomedical Functional Materials and Jiangsu Key Laboratory of Biofunctional Materials, School of Chemistry and Materials Science, Nanjing Normal University, Nanjing 210023, P. R. China. E-mail: daizhihuii@njnu.edu.cn; Fax: +86-25-85891051; Tel: +86-25-85891051

† Electronic supplementary information (ESI) available: Experimental methods, optimization of detection conditions, electrochemical performance and analysis of real samples. See DOI: 10.1039/c4cc03555k

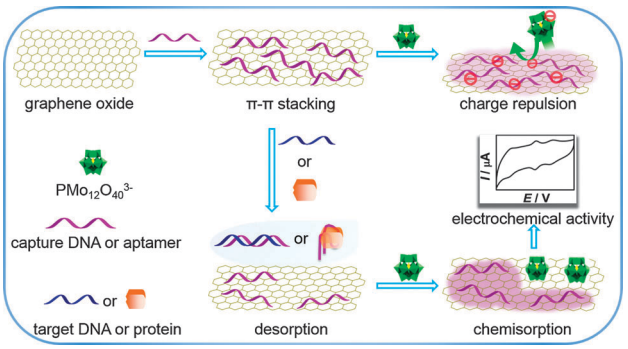

Scheme 1 Schematic representation of the label-free electrochemical biosensing platform for DNA and protein analysis based on PMo_{12}.

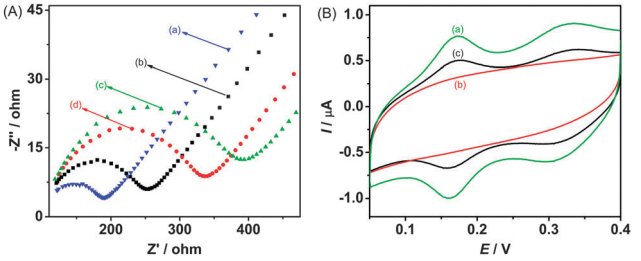

Fig. 1 (A) Nyquist diagrams of (a) GCE/chitosan, (b) GCE/chitosan/GO, (c) GCE/chitosan/GO/DNA1 and (d) GCE/chitosan/GO/DNA1/DNA2 in 10 mM $[Fe(CN)_6]^{3-/4-}$ solution containing 0.1 M KCl. (B) Cyclic voltammograms (CVs) obtained at (a) GCE/chitosan/GO/PMo_{12}, (b) GCE/chitosan/GO/DNA1/PMo_{12}, (c) GCE/chitosan/GO/DNA1/DNA2/PMo_{12} electrodes in 0.5 M H_2SO_4 solution containing 0.1 M NaCl.

double-stranded DNA or aptamer–protein complexes are released from the conjugated interface of GO, thus leaving some space for PMo_{12} to anchor. Owing to the chemisorption between GO and POM,[7a] PMo_{12} could steadily attach to the GO surface. Finally, by taking advantage of the electrochemical activity of the adherent PMo_{12} (ref. 12) and the positive correlation between the concentration of the target and the PMo_{12}, the content of the detection target can be easily analysed.

The morphologies of chitosan, chitosan/GO, chitosan/GO/ DNA1/ PMo_{12} and chitosan/GO/DNA1/DNA2/ PMo_{12} films (Fig. S2, ESI†) were characterized by scanning electron microscopy (SEM). The surface of chitosan/GO showed that the slightly wrinkled GO covered the uneven chitosan like a soft gauze (Fig. S2B, ESI†), while the surface of chitosan/GO/DNA1/DNA2/PMo_{12} (Fig. S2D, ESI†) became more inhomogeneous and rough, which might be due to immobilization of DNA1 and PMo_{12}. In order to verify the verdict, energy dispersive spectroscopy (EDS) analysis was performed (insets in Fig. S2, ESI†). The presence of Mo atoms and the decreasing ratios of C/O atoms (insets in Fig. S2D, ESI†) indicated that a small amount of PMo_{12} had been adsorbed on the surface of chitosan–GO.

The stepwise assembly process of the biosensing interface was investigated by electrochemical impedance spectroscopy (EIS). EIS is being increasingly used to monitor the DNA immobilization and hybridization process because of its ability to probe the properties of the interfacial electron transfer.[13] The Nyquist plots of GCE/chitosan (a), GCE/chitosan/GO (b), GCE/chitosan/GO/capture single-stranded DNA (DNA1) (c), and GCE/chitosan/GO/DNA1/target DNA (DNA2) (d) using $[Fe(CN)_6]^{3-/4-}$ as the indicator are shown in Fig. 1A. The diameter of the semicircle was equal to the charge-transfer resistance (R_{ct}). The impedance spectra showed a lowest R_{ct} value (70 Ω) for the bare GCE/chitosan electrode (Fig. 1A, curve a). The R_{ct} value presented by curve b (133 Ω) increased with GO coating. The results demonstrated that the low electrical conductivity of GO blocked the electron transfer of $[Fe(CN)_6]^{3-/4-}$.[14] Then curve c presented a larger R_{ct} value (279 Ω) compared with curve b, suggesting efficient immobilization of DNA1 on the GCE/chitosan/GO surface. Compared with curve c, when DNA2 was added on the surface of the GCE/chitosan/GO/DNA1 electrode, the binding between DNA1 and target DNA2 altered the conformation of DNA1 and disturbed the interaction between DNA1 and GO.[10a] The DNA duplex formed was released from the surface of GO and washed away from the electrode. Therefore, a significant decrease of the R_{ct} value (212 Ω) was observed (curve d). These changes in the EIS indicated the efficient immobilization and hybridization of DNA on the surface of GO and confirmed the successful fabrication of the biosensing interface.

The cyclic voltammograms (CVs) of GCE/chitosan/GO/PMo_{12} (see ESI,† Fig. S3) were recorded to investigate the interaction between GO and POM. The CVs of GCE/chitosan/GO/PMo_{12} showed three reversible pairs of redox peaks at different scan rates (ν) (Fig. S3A, ESI†). The peak currents for three pairs of redox peaks increased linearly with different ν from 10 to 100 mV s^{-1} (Fig. S3B, ESI†), indicating a surface-controlled redox process. This phenomenon confirmed the existing chemisorption between GO and POM. 50 mV s^{-1} was selected as the scan rate for subsequent tests in view of the noise. The current of peak III was so small that peaks I and II were chosen as the research object in CVs and square wave pulse voltammetric (SWV) analysis.

To further confirm the mutual electrostatic repulsion of PMo_{12} towards DNA1, CVs were scanned. As shown in Fig. 1B, two pairs of well-defined peaks were observed for the GCE/chitosan/GO/PMo_{12} electrode (curve a), which were ascribed to the redox process of PMo_{12}.[6] The addition of 1 μM DNA1 on the GCE/chitosan/GO surface followed by PMo_{12} incubation resulted in the disappearance of the redox peaks (curve b). This is due to the fact that negative charges on the phosphate backbone of the immobilized DNA1 can form the DNA probe film, which introduced steric hindrance and repelled the negatively charged redox probe.[13b,15] Therefore the adhesion of PMo_{12} on GO was greatly reduced due to the steric hindrance and electrostatic repulsion. After hybridization with DNA2, the electrode surface was incubated with PMo_{12}, and the redox peaks were recovered (curve c), suggesting that the resulting double-stranded DNA was released from the conjugated interface of GO, leaving some space for PMo_{12} to anchor.

Under the optimized conditions (1 μM DNA1, 2 h of DNA hybridization time, 50 min of PMo_{12} incubation time and 50 μM PMo_{12}) (see ESI,† Fig. S4), the SWV peak currents increased with the increasing concentrations of DNA2 (Fig. 2A). As shown in the inset graph of Fig. 2A, the I_p for the reduction peak II of PMo_{12} (I_{pII}) was proportional to the logarithm of the DNA2 concentration from

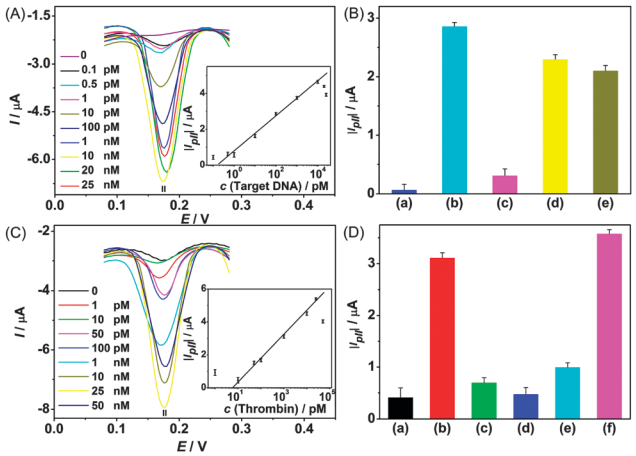

Fig. 2 Typical SWV curves of the electrochemical assay using PMo_{12} as a probe with increasing concentrations of (A) DNA2 and (C) thrombin. Inset: calibration curves. (B) Specificity of the gene sensor investigated with (a) 0 pM DNA2, (b) 100 pM DNA2, (c) 100 pM random sequence (DNA3), (d) 100 pM single-base mismatched target sequence (DNA4) and (e) 100 pM mutant type target sequence (DNA5). (D) Selectivity analysis of the protein sensor tested in (a) blank solution, (b) 1 nM thrombin, (c) 1 μM BSA, (d) 1 μM Hb, (e) 1 μM HSA and (f) 1 nM thrombin with 1μM BSA, 1 μM Hb and 1 μM HSA.

0.5 pM to 10 nM. The detection limit for DNA2 was 0.2 pM, which was obtained by using the slope of the linear part of the curve and dividing by 3σ (10 negative controls processed with PMo_{12} and in the absence of target DNA). The linear range and detection limit were better than those obtained using other modified electrodes and methods (see ESI,† Table S1). GCE/chitosan/GO/DNA1 was hybridized with different DNA sequences to test the selectivity and usability of the biosensor for DNA analysis. The $|I_{pII}|$ was used to estimate the efficiency of DNA hybridization. As shown in Fig. 2B, DNA2 showed higher $|I_{pII}|$ compared with random sequences (Fig. 2B, column c), a single-base mismatched sequence (Fig. 2B, column d) and a mutant sequence (Fig. 2B, column e). The results clearly demonstrated that the prepared DNA biosensor had a good selectivity for the detection of target DNA sequence, and the discrimination ability for noncomplementary DNA was better than that for single-base mismatch and mutant sequences. The resulting PMo_{12}-based DNA sensor was also scanned in 0.5 M H_2SO_4 containing 0.1 M NaCl solution from 0.05 to 0.4 V at 50 mV s^{-1} for 20 cycles (Fig. S5, ESI†). The peak currents were stable, suggesting good stability of the biosensor. We also investigated the stability in the absence of chitosan (see ESI,† Fig. S6), the current decreased sharply during the electrochemical test, indicating the important role of chitosan.

In the meantime, the platform was used for the detection of proteins (human thrombin as a model) to test its generality. An equal amount of the human thrombin aptamer was used to replace DNA1. Fig. 2C shows SWV curves at different thrombin concentrations. In the inset graph of Fig. 2C, the $|I_{pII}|$ was proportional to the logarithm of the thrombin concentration from 10 pM to 25 nM. The detection limit for thrombin was 5.8 pM, which was obtained by using the slope of the linear part of the curve and dividing by 3σ (10 negative controls processed with PMo_{12} and in the absence of thrombin). The linear range and detection limit were better than those observed of other modified electrodes and methods (see ESI,† Table S2). Meanwhile, bovine serum albumin (BSA), hemoglobin (Hb) and human serum albumin (HSA) were selected to study the specificity. A significant current response was observed for thrombin (see Fig. 2D(b)), while little change in I_{pII} was observed for 1 μM BSA, Hb and HSA. The good selectivity for thrombin is attributed to the high specificity of the aptamer. Comparing with thrombin alone, the current increased by only 15% in the mixed sample (see Fig. 2D(f)). The experiment verified the good selectivity of the biosensor for thrombin detection. Furthermore, the results obtained from real serum sample measurements validated the feasibility of the proposed electrochemical biosensing strategy (see ESI,† Table S3).

In summary, a versatile label-free, stable, low-cost and simple electrochemical biosensing platform for the detection of DNA and proteins was developed by jointly taking advantages of electronegativity and electrochemical activity of PMo_{12}, and its chemisorption with GO. Using a disease-related gene sequence (mitochondrial DNA related to maternally inherited diabetes) and the thrombin as models, the platform was applied to the analysis of DNA and proteins. DNA assay and quantitative determination of thrombin in human blood was realized and satisfactory results were achieved. The novel POM based electrochemical biosensing platform would have a promising prospect in clinical diagnosis.

This work was supported by the National Natural Science Foundation of China (21175069 and 21205061). We appreciate the financial support from the Priority Academic Program Development of Jiangsu Higher Education Institutions.

Notes and references

1 (*a*) P. A. Sontz, T. P. Mui, J. O. Fuss, J. A. Tainer and J. K. Barton, *Proc. Natl. Acad. Sci. U. S. A.*, 2012, **109**, 1856; (*b*) S. J. Kwon and A. J. Bard, *J. Am. Chem. Soc.*, 2012, **134**, 10777; (*c*) E. Palecek and M. Bartosik, *Chem. Rev.*, 2012, **112**, 3427.
2 (*a*) Q. P. Wang, H. Y. Zheng, X. Y. Gao, Z. Y. Lin and G. N. Chen, *Chem. Commun.*, 2013, **49**, 11418; (*b*) S. Martic, M. Gabriel, J. P. Turowec, D. W. Litchfield and H. B. Kraatz, *J. Am. Chem. Soc.*, 2012, **134**, 17036; (*c*) B. Farrow, S. A. Hong, E. C. Romero, B. Lai, M. B. Coppock, K. M. Deyle, A. S. Finch, D. N. Stratis-Cullum, H. D. Agnew, S. Yang and J. R. Heath, *ACS Nano*, 2013, **7**, 9452.
3 (*a*) F. Y. Kong, B. Y. Xu, Y. Du, J. J. Xu and H. Y. Chen, *Chem. Commun.*, 2013, **49**, 1052; (*b*) X. Y. Lang, H. Y. Fu, C. Hou, G. F. Han, P. Yang, Y. B. Liu and Q. Jiang, *Nat. Commun.*, 2013, **4**, 2169; (*c*) X. L. Chai, X. G. Zhou, A. W. Zhu, L. M. Zhang, Y. Qin, G. Y. Shi and Y. Tian, *Angew. Chem., Int. Ed.*, 2013, **52**, 8129; (*d*) Y. Q. Ren, H. M. Deng, W. Shen and Z. Q. Gao, *Anal. Chem.*, 2013, **85**, 4784.
4 (*a*) D. L. Long, R. Tsunashima and L. Cronin, *Angew. Chem., Int. Ed.*, 2010, **49**, 1736; (*b*) J. Geng, M. Li, J. S. Ren, E. B. Wang and X. G. Qu, *Angew. Chem., Int. Ed.*, 2011, **123**, 4270.
5 (*a*) H. L. Li, S. P. Pang, S. Wu, X. L. Feng, K. Mullen and C. Bubeck, *J. Am. Chem. Soc.*, 2011, **133**, 9423; (*b*) Y. F. Song and R. Tsunashima, *Chem. Soc. Rev.*, 2012, **41**, 7384.
6 (*a*) N. Kawasaki, H. Wang, R. Nakanishi, S. Hamanaka, R. Kitaura, H. Shinohara, T. Yokoyama, H. Yoshikawa and K. Awaga, *Angew. Chem., Int. Ed.*, 2011, **123**, 3533; (*b*) C. Rinfray, G. Izzet, J. Pinson, S. G. Derouich, J. J. Ganem, C. Combellas, F. Kanoufi and A. Proust, *Chem. – Eur. J.*, 2013, **19**, 13838.
7 (*a*) D. Zhou and B. H. Han, *Adv. Funct. Mater.*, 2010, **20**, 2717; (*b*) J. P. Tessonnier, S. Goubert-Renaudin, S. Alia, Y. S. Yan and M. A. Barteau, *Langmuir*, 2013, **29**, 393.

8 R. P. Johnson, J. A. Richardson, T. Brown and P. N. Bartlett, *J. Am. Chem. Soc.*, 2012, **134**, 14099.
9 (*a*) C. Li, Z. Y. Wang, T. Gao, A. P. Duan and G. X. Li, *Chem. Commun.*, 2013, **49**, 3760; (*b*) T. Kurkina, A. Vlandas, A. Ahmad, K. Kern and K. Balasubramanian, *Angew. Chem., Int. Ed.*, 2011, **50**, 3710; (*c*) T. Bryan, X. L. Luo, P. R. Bueno and J. J. Davis, *Biosens. Bioelectron.*, 2013, **39**, 94.
10 (*a*) C. H. Lu, H. H. Yang, C. L. Zhu, X. Chen and G. N. Chen, *Angew. Chem., Int. Ed.*, 2009, **121**, 4879; (*b*) M. Muti, S. Sharma, A. Erdem and P. Papakonstantinou, *Electroanalysis*, 2011, **23**, 272; (*c*) L. H. Tang, Y. Wang, Y. Liu and J. H. Li, *ACS Nano*, 2011, **5**, 3817.
11 (*a*) T. Chandy and C. P. Sharma, *Biomater., Artif. Cells, Artif. Organs*, 1990, **18**, 1; (*b*) W. Paul and C. P. Sharma, *STP Pharma Sci.*, 2000, **10**, 5; (*c*) R. A. A. Muzzarelli and C. Muzzarelli, *Adv. Polym. Sci.*, 2005, **186**, 151; (*d*) A. Erdem, E. Eksin and M. Muti, *Colloids Surf., B*, 2014, **115**, 205.
12 J. Chen, S. L. Liu, W. Feng, G. Q. Zhang and F. L. Yang, *Phys. Chem. Chem. Phys.*, 2013, **15**, 5664.
13 (*a*) T. Yang, Q. H. Li, X. Li, X. H. Wang, M. Du and K. Jiao, *Biosens. Bioelectron.*, 2013, **42**, 415; (*b*) A. Bonanni and M. Pumera, *ACS Nano*, 2011, **5**, 2356.
14 (*a*) T. Yang, Q. Guan, X. H. Guo, L. Meng, M. Du and K. Jiao, *Anal. Chem.*, 2013, **85**, 1358; (*b*) S. Stankovich, R. D. Piner, X. Q. Chen, N. Q. Wu, S. T. Nguyen and R. S. Ruoff, *J. Mater. Chem.*, 2006, **16**, 155.
15 B. Pejcic and R. De Marco, *Electrochim. Acta*, 2006, **51**, 6217.

